

# An Improved Bound on the Optimal Paper Moebius Band

Richard Evan Schwartz <sup>\*</sup>

October 9, 2020

## Abstract

We show that a smooth embedded paper Moebius band must have aspect ratio at least

$$\lambda_1 = \frac{2\sqrt{4 - 2\sqrt{3}} + 4}{\sqrt[4]{3}\sqrt{2} + 2\sqrt{2\sqrt{3} - 3}} = 1.69497\dots$$

This bound comes more than 3/4 of the way from the old known bound of  $\pi/2 = 1.5708\dots$  to the conjectured bound of  $\sqrt{3} = 1.732\dots$ . We also prove some refinements and variants of our basic bound.

## 1 Introduction

This paper addresses the following question. *What is the aspect ratio of the shortest smooth paper Moebius band?* Let's state the basic question more precisely. Given  $\lambda > 0$ , let

$$M_\lambda = ([0, 1] \times [0, \lambda]) / \sim, \quad (x, 0) \sim (1 - x, \lambda) \quad (1)$$

denote the standard flat Moebius band of width 1 and height  $\lambda$ . This Moebius band has aspect ratio  $\lambda$ . Let  $S \subset \mathbf{R}_+$  denote the set of values of  $\lambda$  such that

---

<sup>\*</sup>Supported by N.S.F. Grant DMS-1807320

there is a smooth<sup>1</sup> isometric embedding  $I : M_\lambda \rightarrow \mathbf{R}^3$ . The question above asks for the quantity

$$\lambda_0 = \inf S. \quad (2)$$

The best known result, due to Halpern and Weaver [HW], is that

$$\lambda_0 \in [\pi/2, \sqrt{3}]. \quad (3)$$

In §14 of their book, *Mathematical Omnibus* [FT], Fuchs and Tabachnikov give a beautiful exposition of the problems and these bounds. This is where I learned about the problem.

The lower bound is local in nature and does not see the difference between immersions and embeddings. Indeed, in [FT], a sequence of immersed examples whose aspect ratio tends to  $\pi/2$  is given. The upper bound comes from an explicit construction. The left side of Figure 1.1 shows  $M_{\sqrt{3}}$ , together with a certain union of *bends* drawn on it. The right side shows the nearly embedded paper Moebius band one gets by folding this paper model up according to the bending lines.

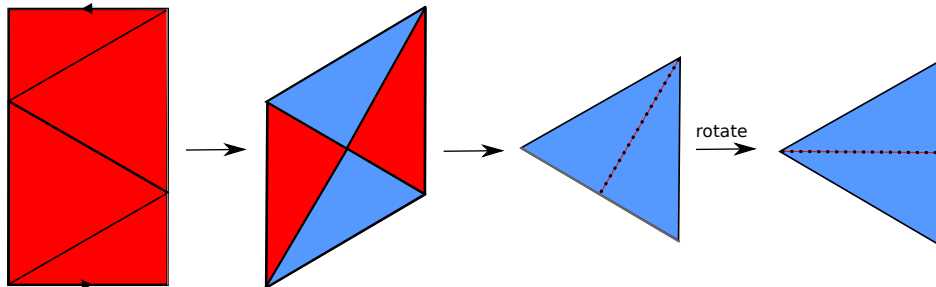


**Figure 1.1:** The conjectured optimal paper Moebius band

The Moebius band just described is degenerate: It coincides as a set with the equilateral triangle  $\Delta$  of semi-perimeter  $\sqrt{3}$ . However, one can choose any  $\epsilon > 0$  and find a nearby smoothly embedded image of  $M_{\sqrt{3}+\epsilon}$  by a process of rounding out the folds and slightly separating the sheets. Halpern and

---

<sup>1</sup>The smoothness requirement (or some suitable variant) is necessary in order to have a nontrivial problem. Given any  $\epsilon > 0$ , one can start with the strip  $[0, 1] \times [0, \epsilon]$  and first fold it (across vertical folds) so that it becomes, say, an  $(\epsilon/100) \times \epsilon$  “accordion”. One can then easily twist this “accordion” once around in space so that it makes a Moebius band. The corresponding map from  $M_\epsilon$  is an isometry but it cannot be approximated by smooth isometric embeddings.

Weaver conjecture that  $\lambda_0 = \sqrt{3}$ , so that the triangular example is the best one can do.

The Moebius band question in a sense goes back a long time, and it is related to many topics. The early paper [Sa] proves rigorously that smooth paper Moebius bands exist. (See [HF] for a modern translation to english.) The paper [CF] gives a general framework for considering the differential geometry of developable surfaces. Some authors have discussed optimal shapes for Moebius bands from other perspectives, e.g. algebraic or physical. See, e.g. [MK] and [S1]. The Moebius band question has connections to origami. See e.g. the beautiful examples of isometrically embedded flat tori [AHLM]. It is also related to the main optimization question from geometric knot theory: What is the shortest piece rope one can use to tie a given knot? See e.g. [CKS]. Finally (as we discuss in §5) the Moebius band question related to topics in discrete computational geometry such as tensegrities [CB].

In this paper we improve the lower bound.

**Theorem 1.1 (Main)** *An embedded paper Moebius band must have aspect ratio at least*

$$\lambda_1 = \frac{2\sqrt{4 - 2\sqrt{3}} + 4}{\sqrt[4]{3}\sqrt{2} + 2\sqrt{2\sqrt{3} - 3}} = 1.69497\dots$$

This value  $\lambda_1$  arises naturally in a geometric optimization problem involving trapezoids. To quantify the way that our result improves over the previous lower bound, we note that  $\lambda_1 > \sqrt{3} - (1/26)$  whereas  $\pi/2 < \sqrt{3} - (4/26)$ .

The proof of the Main Theorem has 2 ideas, which we now explain. Being a ruled surface,  $I(M_\lambda)$  contains a continuous family of line segments which have their endpoints on  $\partial I(M_\lambda)$ . We call these line segments *bend images*. Say that a *T-pattern* is a pair of perpendicular coplanar bend images. The T-pattern looks somewhat like the two vertical and horizontal segments on the right side of Figure 1.1 except that the two segments are disjoint in an embedded example. Here is our first idea.

**Lemma 1.2** *An embedded paper Moebius band of aspect ratio less than  $7\pi/12$  contains a T-pattern.*

Note that  $7\pi/12 > \sqrt{3}$ , so Lemma 1.2 applies to the examples of interest to us. Lemma 1.2 relies crucially on the embedding property. The immersed examples in [FT] do not have these T-patterns.

The two bend images comprising the  $T$ -pattern divide  $I(M)$  into two halves. Our second idea is to observe that the image  $I(\partial M_\lambda)$  makes a loop which hits all the vertices of the  $T$ -pattern. When we compare the relevant portions of  $\partial M_\lambda$  with a polygon made from the vertices of the  $T$ -pattern, we get two constraints which lead naturally to the lower bound of  $\lambda_1$ .

Since we can almost effortlessly give *some* improvement to the lower bound using Lemma 1.2, we do this now. The convex hull of the  $T$ -pattern contains a triangle of base at least 1 and height at least 1. Such a triangle has semi-perimeter at least  $\phi = 1.61\dots$ , the golden ratio. Hence  $\lambda_0 \geq \phi$ . The argument which gives  $\lambda_0 \geq \lambda_1$ , the constant in Theorem 1.1, is similar in spirit but more elaborate.

It would have been nice if the existence of a  $T$ -pattern forced  $\lambda > \sqrt{3}$  on its own. This is not the case. In Figure 2.1 we show half of an immersed paper Moebius band of aspect ratio less than  $\sqrt{3}$  that has a  $T$ -pattern. I did not try to formally prove that these exist, but using my computer program I can construct them easily. I will sketch a finite dimensional calculation which, if completed, would show that an immersed paper Moebius band with a  $T$ -pattern has aspect ratio at least  $\sqrt{3} - (1/58) = 1.7148\dots$  This would significantly improve the bound in Theorem 1.1, but I don't know how to make the calculation feasible.

This paper is organized as follows. In §2 we introduce some basic geometric objects associated to a paper Moebius band and the prove Lemma 1.2. In §3 we give the argument involving the vertices of the  $T$ -pattern and thereby prove Theorem 1.1. In §4 we prove Theorem 4.1, a result which refines Theorem 1.1 in some sense. For instance, one of the statements in Theorem 4.1 is that the convex hull of the  $T$ -pattern is a triangle with all angles exceeding  $\pi/4$ .

I would like to thank Sergei Tabachnikov for telling me about this problem and for helpful discussions about it. I would also like to thank the Simons Foundation and the Institute for Advanced Study for their support during my 2020-21 sabbatical.

## 2 Existence of the T Pattern

### 2.1 Polygonal Moebius Bands

**Basic Definition:** Say that a *polygonal Moebius band* is a pair  $\mathcal{M} = (\lambda, I)$  where  $I : M_\lambda \rightarrow \mathbf{R}^3$  is an isometric embedding that is affine on each triangle of a triangulation of  $M_\lambda$ . We insist that the vertices of these triangles all lie on  $\partial M_\lambda$ , as in Figure 1.1. Any smooth isometric embedding  $I' : M_\lambda \rightarrow \mathbf{R}^3$  can be approximated arbitrarily closely by this kind of map, so it suffices to work entirely with polygonal Moebius bands.

**Associated Objects:** Let  $\delta_1, \dots, \delta_n$  be the successive triangles of  $\mathcal{M}$ .

- The *ridge* of  $\delta_i$  is edge of  $\delta_i$  that is contained in  $\partial M_\lambda$ .
- The *apex* of  $\delta_i$  to be the vertex of  $\delta_i$  opposite the ridge.
- A *bend* is a line segment of  $\delta_i$  connecting the apex to a ridge point.
- A *bend image* is the image of a bend under  $I$ .
- A *facet* is the image of some  $\delta_i$  under  $I$ .

We always represent  $M_\lambda$  as a parallelogram with top and bottom sides identified. We do this by cutting  $M_\lambda$  open at a bend. See Figure 2.1 below.

**The Sign Sequence:** Let  $\delta_1, \dots, \delta_n$  be the triangles of the triangulation associated to  $\mathcal{M}$ , going from bottom to top in  $P_\lambda$ . We define  $\mu_i = -1$  if  $\delta_i$  has its ridge on the left edge of  $P_\lambda$  and  $+1$  if the ridge is on the right. The sequence for the example in Figure 1.1 is  $+1, -1, +1, -1$ .

**The Core Curve:** There is a circle  $\gamma$  in  $M_\lambda$  which stays parallel to the boundary and exactly  $1/2$  units away. In Equation 1, this circle is the image of  $\{1/2\} \times [0, \lambda]$  under the quotient map. We call  $I(\gamma)$  the *core curve*.

The left side of Figure 2.1 shows  $M_\lambda$  and the pattern of bends. The vertical white segment is the bottom half of  $\gamma$ . The right side of Figure 2.1 (which has been magnified to show it better) shows  $I(\tau)$  where  $\tau$  is the colored half of  $M_\lambda$ . All bend angles are  $\pi$  and the whole picture is planar. The colored curve on the right is the corresponding half of the core curve. Incidentally, for  $\tau$  we have  $L + R = 1.72121\dots < \sqrt{3}$ .

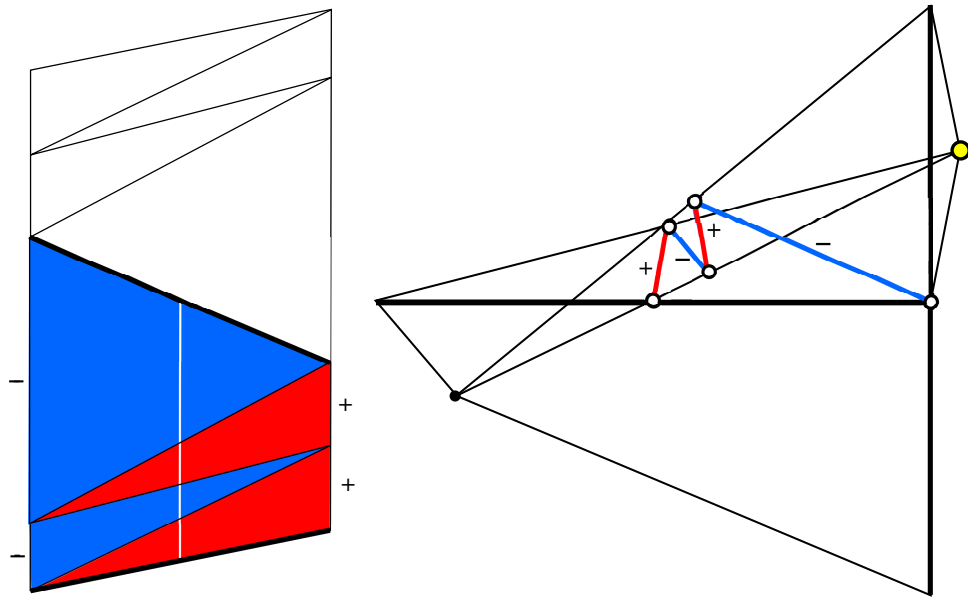


**Figure 2.1:** The bend pattern and the bottom half of the image

**The Ridge Curve:** We show the picture first, then explain.

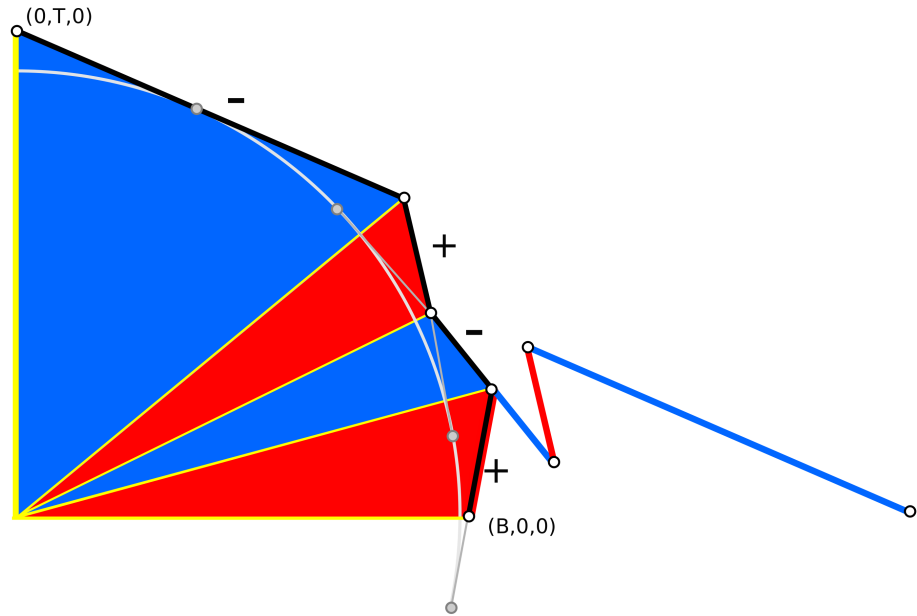


**Figure 2.2:** Half 2x core curve (red/blue) and half ridge curve (black).

Let  $\beta_b$  be the bottom edge of the parallelogram representing  $M_\lambda$ . We normalize so that  $I$  maps the left vertex of  $\beta_b$  to  $(0, 0, 0)$  and the right vertex to  $(B, 0, 0)$ , where  $B$  is the length of  $\beta_b$ . Let  $E_1, \dots, E_n$  be the successive edges of the core curve, treated as vectors. Let

$$\Gamma'_i = 2\mu_i E_i, \quad i = 1, \dots, n. \quad (4)$$

Let  $\Gamma$  be the curve whose initial vertex is  $(B, 0, 0)$  and whose edges are  $\Gamma'_1, \dots, \Gamma'_n$ . Here  $\mu_1, \dots, \mu_n$  is the sign sequence.

$\Gamma$  has length  $2\lambda$ , connects  $(B, 0, 0)$  to  $(-B, 0, 0)$ , and is disjoint from the open unit ball. The lines extending the sides of  $\Gamma$  are tangent to the unit sphere. We rotate so that  $\Gamma$  contains  $(0, T, 0)$  for some  $T > 1$ . If we cone  $\Gamma$  to the origin, we get a collection  $\Delta_1, \dots, \Delta_n$  of triangles, and  $\Delta_i$  is the translate of  $\mu_i I(\delta_i)$  whose apex is at the origin. In particular, the vectors pointing to the vertices of  $\Gamma$  are parallel to the corresponding bend images. Figure 2.2 shows the portion of the ridge curve (in black) associated to the example in Figure 2.1. We have also scaled the core curve by 2 and translated it to show the relationships between the two curves.

## 2.2 Geometric Bounds

While we are in the neighborhood, we re-prove the lower bound from [FT]. The proof in [FT] is somewhat similar, though it does not use the ridge curve. Let  $\lambda$  be the aspect of the polygonal Moebius band  $\mathcal{M}$  and let  $\Gamma$  be the associated ridge curve. Let  $f : \mathbf{R}^3 - B^3 \rightarrow S^2$  be orthogonal projection. The map  $f$  is arc-length decreasing. Letting  $\Gamma^* = f(\Gamma)$ , we have  $|\Gamma^*| < |\Gamma| = 2\lambda$ . Since  $\Gamma^*$  connects a point on  $S^2$  to its antipode,  $|\Gamma^*| \geq \pi$ . Hence  $\lambda > \pi/2$ .

Now we use the same idea in a different way.

**Lemma 2.1** *Suppose  $\mathcal{M}$  has aspect ratio less than  $7\pi/12$ . Then the ridge curve  $\Gamma$  lies in the open slab bounded by the planes  $Z = \pm 1/\sqrt{2}$ .*

**Proof:** We divide  $\Gamma$  into halves. One half goes from  $(B, 0, 0)$  to  $(0, T, 0)$  and the second half goes from  $(0, T, 0)$  to  $(-B, 0, 0)$ . Call the first half  $\Gamma_1$ . Suppose that  $\Gamma_1$  intersects the plane  $Z = 1/\sqrt{2}$ . Then the spherical projection  $\Gamma_1^*$  goes from  $A = (1, 0, 0)$  to some unit vector  $B = (u, v, 1/\sqrt{2})$  to  $C = (0, 1, 0)$ . Here  $u^2 + v^2 = 1/2$ . The shortest path like this is the geodesic bigon connecting  $A$  to  $B$  to  $C$ . Such a bigon has length at least

$$\arccos(A \cdot B) + \arccos(B \cdot C) = \arccos(u) + \arccos(v) \geq^* 2 \arccos(1/2) = 2\pi/3.$$

The starred inequality comes from the fact that the minimum, subject to the constraint  $u^2 + v^2 = 1/2$ , occurs at  $u = v = 1/2$ .

But then  $\Gamma$  has length at least  $2\pi/3 + \pi/2 = 7\pi/6$ . This exceeds twice the aspect ratio of  $\mathcal{M}$ . This is a contradiction. The same argument works if  $\Gamma_1$  hits the plane  $Z = -1/\sqrt{2}$ . Likewise the same argument works with the second half of  $\Gamma$  in place of the first half. ♠

**Corollary 2.2** *Suppose  $\mathcal{M}$  has aspect ratio less than  $7\pi/12$ . Let  $\beta_1^*$  and  $\beta_2^*$  be two perpendicular bend images. Then a plane parallel to both  $\beta_1^*$  and  $\beta_2^*$  cannot contain a vertical line.*

**Proof:** Every bend image is parallel to some vector from the origin to a point of  $\Gamma$ . By the previous result, such a vector make an angle of less than  $\pi/4$  with the  $XY$ -plane. Hence, all bend images make angles of less than  $\pi/4$  with the  $XY$ -plane. Suppose our claim is false. Since  $\beta_1^*$  and  $\beta_2^*$  are perpendicular to each other, one of them must make an angle of at least  $\pi/4$  with the  $XY$ -plane. This is a contradiction. ♠

### 2.3 Perpendicular Lines

As a prelude to the work in the next section, we prove a few results about lines and planes. Say that an *anchored line* in  $\mathbf{R}^3$  is a line through the origin. Let  $\Pi_1$  and  $\Pi_2$  be planes through the origin in  $\mathbf{R}^3$ .

**Lemma 2.3** *Suppose that  $\Pi_1$  and  $\Pi_2$  are not perpendicular. The set of perpendicular anchored lines  $(L_1, L_2)$  with  $L_j \in P_j$  for  $j = 1, 2$  is diffeomorphic to a circle.*

**Proof:** For each anchored line  $L_1 \in \Pi_1$  the line  $L_2 = L_1^\perp \cap \Pi_2$  is the unique choice anchored line in  $\Pi_2$  which is perpendicular to  $L_1$ . The line  $L_2$  is a smooth function of  $L_1$ . So, the map  $(L_1, L_2) \rightarrow L_1$  gives a diffeomorphism between the space of interest to us and a circle. ♠

A *sector* of the plane  $\Pi_j$  is a set linearly equivalent to the union of the  $(++)$  and  $(--)$  quadrants in  $\mathbf{R}^2$ . Let  $\Sigma_j \subset \Pi_j$  be a sector. The boundary  $\partial\Sigma_j$  is a union of two anchored lines.

**Lemma 2.4** *Suppose (again) that the planes  $\Pi_1$  and  $\Pi_2$  are not perpendicular. Suppose also that no line of  $\partial\Sigma_1$  is perpendicular to a line of  $\partial\Sigma_2$ . Then the set of perpendicular pairs of anchored lines  $(L_1, L_2)$  with  $L_j \in \Sigma_j$  for  $j = 1, 2$  is either empty or diffeomorphic to a closed line segment.*

**Proof:** Let  $S^1$  denote the set of perpendicular pairs as in Lemma 2.3. Let  $X \subset S^1$  denote the set of those pairs with  $L_j \in \Sigma_j$ . Let  $\pi_1$  and  $\pi_2$  be the two diffeomorphisms from Lemma 2.3. The set of anchored lines in  $\Sigma_j$  is a line segment and hence so is its inverse image  $X_j \subset S^1$  under  $\pi_j$ . We have  $X = X_1 \cap X_2$ . Suppose  $X$  is nonempty. Then some  $p \in X$  corresponds to a pair of lines  $(L_1, L_2)$  with at most one  $L_j \in \partial\Sigma_j$ . But then we can perturb  $p$  slightly, in at least one direction, so that the corresponding pair of lines remains in  $\Sigma_1 \times \Sigma_2$ . This shows that  $X_1 \cap X_2$ , if nonempty, contains more than one point. But then the only possibility, given that both  $X_1$  and  $X_2$  are segments, is that their intersection is also a segment. ♠

## 2.4 The Space of Perpendicular Pairs

We prove the results in this section more generally for piecewise affine maps  $I : M_\lambda \rightarrow \mathbf{R}^3$  which are not necessarily local isometries. The reason for the added generality is that it is easier to make perturbations within this category. Let  $\mathbf{X}$  be the space of such maps which also satisfy the conclusion of Corollary 2.2. (In this section we will not use this property but in the next section we will.) So,  $\mathbf{X}$  includes all (isometric) polygonal Moebius bands of aspect ratio less than  $7\pi/12$ . The notions of bend images and facets makes sense for members of  $\mathbf{X}$ .

**Lemma 2.5** *The space  $\mathbf{X}$  has a dense set  $\mathbf{Y}$  which consists of members such that no two facets lie in perpendicular planes and no two special bend images are perpendicular.*

**Proof:** One can start with any member of  $\mathbf{X}$  and postcompose the whole map with a linear transformation arbitrarily close to the identity so as to get a member of  $\mathbf{Y}$ . The point is that we just need to destroy finitely many perpendicularity relations. ♠

Let  $\gamma$  be center circle of  $M_\lambda$ . We can identify the space of bend images of  $\mathcal{M}$  with  $\gamma$ : The bends and bend-images are in bijection, and each bend intersects  $\gamma$  once. The space of ordered pairs of unequal bend images can be identified with  $\gamma \times \gamma$  minus the diagonal. We compactify this space by adding in 2 boundary components. One of the boundary components comes from approaching the main diagonal from one side and the other comes from approaching the diagonal from the other side. The resulting space  $A$  is an annulus. For the rest of the section we choose a member of  $\mathbf{Y}$  and make all definitions for this member.

**Lemma 2.6**  $\mathcal{P}$  is a piecewise smooth 1-manifold in  $A$ .

**Proof:** We apply Lemma 2.4 to the planes through the origin parallel to the facets and to the anchored lines parallel to the bend images within the facets. (Within a single facet the bend images and the corresponding anchored lines are in smooth bijection.) By Lemma 2.4, the space  $\mathcal{P}$  is the union of finitely many smooth connected arcs. Each arc corresponds to an ordered pair of facets which contains at least one point of  $\mathcal{P}$ . Each of these arcs has two endpoints. Each endpoint has the form  $(\beta_1^*, \beta_2^*)$  where exactly one of these bend images is special. Let us say that  $\beta_1^*$  is special. Then  $\beta_1^*$  is the edge between two consecutive facets, and hence  $(\beta_1^*, \beta_2^*)$  is the endpoint of exactly 2 of the arcs. Hence the arcs fit together to make a piecewise smooth 1-manifold. ♠

A component of  $\mathcal{P}$  is *essential* if it separates the boundary components of  $A$ .

**Lemma 2.7**  $\mathcal{P}$  has an odd number of essential components.

**Proof:** An essential component, being embedded, must represent a generator for the first homology  $H_1(A) = \mathbf{Z}$ . By duality, a transverse arc running from one boundary component of  $A$  to the other intersects an essential component an odd number of times and an inessential component an even number of times. Let  $a$  be such an arc. As we move along  $a$  the angle between the corresponding bends can be chosen continuously so that it starts at 0 and ends at  $\pi$ . Therefore,  $a$  intersects  $\mathcal{P}$  an odd number of times. But this means that there must be an odd number of essential components of  $\mathcal{P}$ . ♠

## 2.5 The Main Argument

Now we prove Lemma 1.2. Say that a member of  $\mathbf{X}$  is *good* if (with respect to this member) there is a path connected subset  $\mathcal{K} \subset \mathcal{P}$  such that both  $(\beta_1^*, \beta_2^*)$  and  $(\beta_2^*, \beta_1^*)$  belong to  $\mathcal{K}$  for some pair  $(\beta_1^*, \beta_2^*)$ .

**Lemma 2.8** *If  $\mathcal{M}$  is good then  $\mathcal{M}$  has a  $T$ -pattern.*

**Proof:** Each pair  $(\beta_1^*, \beta_2^*)$  in  $\mathcal{P}$  determines a unique pair of parallel planes  $(P_1, P_2)$  such that  $\beta_j^* \subset P_j$  for  $j = 1, 2$ . By hypothesis, members These planes do not contain vertical lines. Hence, our planes intersect the  $Z$ -axis in single and continuously varying points. As we move along  $\mathcal{K}$  these planes exchange places and so do their  $Z$ -intercepts. So, at some instant, the planes coincide and give us a  $T$ -pattern. ♠

**Lemma 2.9** *A dense set of members of  $\mathbf{X}$  are good.*

**Proof:** Let  $\mathbf{Y}$  be the dense subset of  $\mathbf{X}$  considered in the previous section. Relative to any member of  $\mathbf{Y}$ , the space  $\mathcal{P}$  is a piecewise smooth 1-manifold of the annulus  $A$  with an odd number of essential components. The involution  $\iota$ , given by  $\iota(p_1, p_2) = (p_2, p_1)$ , is a continuous involution of  $A$  which preserves  $\mathcal{P}$  and permutes the essential components. Since there are an odd number of these,  $\iota$  preserves some essential component of  $\mathcal{P}$ . But then this essential component contains our set  $\mathcal{K}$ . ♠

Now we know that there are  $T$ -patterns for members of a dense subset of  $\mathbf{X}$ . By compactness and continuity, every member of  $\mathbf{X}$  has a  $T$ -pattern. By Corollary 2.2,  $\mathbf{X}$  contains all (ordinary) embedded polygonal Moebius bands of aspect ratio less than  $7\pi/12$ . Hence all such embedded Moebius bands contain  $T$ -patterns. This completes the proof of Lemma 1.2.

### 3 The Aspect Ratio Bound

#### 3.1 Constraints coming from the T Pattern

Let  $\mathcal{M}$  be a polygonal Moebius band of aspect ratio  $\lambda < 7\pi/12$ . We keep the notation from the previous chapter.

Let  $\beta_1$  and  $\beta_2$  be two bends whose corresponding images  $\beta_1^* = I(\beta_1)$  and  $\beta_2^* = I(\beta_2)$  form a  $T$ -pattern. Since these segments do not intersect, we can label so that the line extending  $\beta_2^*$  does not intersect  $\beta_1^*$ . We cut  $M_\lambda$  open along  $\beta_1$  and treat  $\beta_1$  as the bottom edge. We now set  $\beta_b = \beta_1$  and  $\beta_t = \beta_2$  and (re)normalize as in §2.1. So,  $\beta_b^*$  connects  $(0, 0, 0)$  to  $(B, 0, 0)$ , and  $\beta_t^*$  is a translate of the segment connecting  $(0, 0, 0)$  to  $(0, T, 0)$ . Here  $B$  and  $T$  are the lengths of these segments.

The left side of Figure 3.1 shows  $M_\lambda$ . Reflecting in a vertical line, we normalize so that  $L_1 \geq R_1$ . This means that  $L_2 \geq R_2$ . The right side of Figure 3.1 shows that  $T$  pattern, and the corresponding images of the sets on the left under the isometry  $I$ . The wiggly curves we have drawn do not necessarily lie in the  $XY$ -plane but their endpoints do.

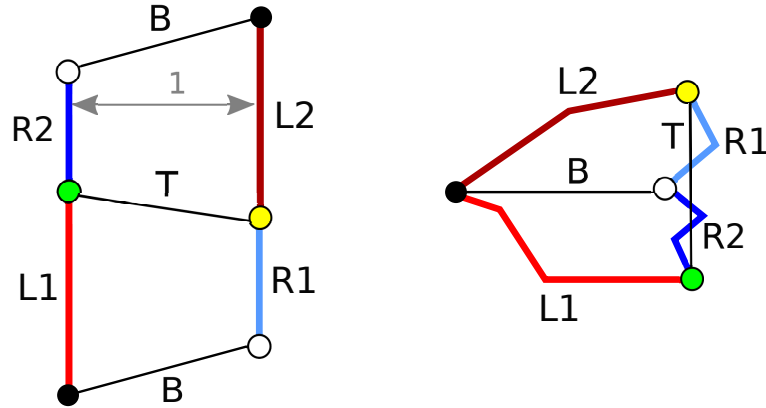


**Figure 3.1:** A Paper Moebius band interacting with the  $T$ -pattern.

There is some  $\epsilon$  such that the vertical distance (i.e., the difference in the  $y$ -coordinates) from the white vertex to the yellow vertex is  $T/2 + \epsilon$  and the vertical distance from the white vertex to the green vertex is  $T/2 - \epsilon$ . Looking at the picture, and using the fact that geodesics in the Euclidean plane are straight lines, we get the following constraints:

$$R_1 + R_1 \geq T, \quad (5)$$

$$L_1 + L_2 \geq \sqrt{B^2 + (T/2 - \epsilon)^2} + \sqrt{B^2 + (T/2 + \epsilon)^2} \geq 2\sqrt{B^2 + T^2/4}. \quad (6)$$

## 3.2 An Optimization Problem

We are done with the Moebius band. We just have a parallelogram as on the left side of Figure 3.1 which satisfies the constraints in Equations 5 and 6 and we want to minimize  $L_1 + L_2 + R_1 + R_2$ . Let  $L = (L_1 + L_2)/2$  and  $R = (R_1 + R_2)/2$ . If we replace  $L_1, L_2$  by  $L, L$  and  $R_1, R_2$  by  $R, R$  the constraints are still satisfied and the sum of interest is unchanged. The constraints now become:

$$2R \geq T, \quad L \geq \sqrt{B^2 + T^2/4}. \quad (7)$$

We show that  $L + R \geq \lambda_1$ , the constant from the Main Theorem, which means

$$\lambda = \frac{1}{2}(L_1 + L_2 + R_1 + R_2) = L + R \geq \lambda_1.$$

So, showing that  $L + R \geq \lambda_1$  finishes the proof of the Main Theorem.

Let  $b$  and  $t$  respectively denote the slopes of the sides labeled  $B$  and  $T$  in Figure 3.2. Let  $S = L + R$ . Since  $L \geq R$  we have  $b \geq t$ . In Figure 3.2 we depict the case when  $b > 0$  and  $t < 0$ . As we see in the next section, this must happen when  $S < \sqrt{3}$ .

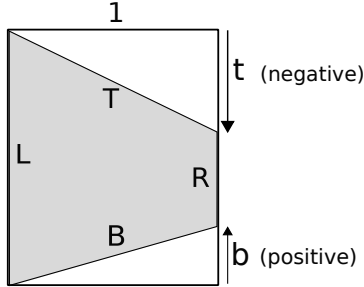


**Figure 3.2:** The basic trapezoid.

Since  $L + R = S$  and  $L - R = b - t$ , and by the Pythagorean Theorem,

$$L = \frac{S + b - t}{2}, \quad R = \frac{S - b + t}{2}, \quad B = \sqrt{1 + b^2}, \quad T = \sqrt{1 + t^2}. \quad (8)$$

Plugging these relations into Equation 7, we get  $S \geq f(b, t)$  and  $S \geq g(b, t)$  where

$$f(b, t) = b - t + T, \quad g(b, t) = -b + t + \sqrt{4B^2 + T^2}.$$

Let  $\phi = \max(f, g)$  and let  $D$  be the domain where  $b \geq t$ . We have  $S \geq \phi$ . To finish the proof of the Main Theorem we just need to show that  $\min_D \phi = \lambda_1$ . This is what we do.

**Lemma 3.1**  $\phi$  achieves its minimum at a point in the interior of  $D$ , and at this point we have  $f = g$ .

**Proof:** We note 3 properties of our functions:

1.  $f(0, -1/\sqrt{3}) = g(0, -1/\sqrt{3}) = \sqrt{3}$ . Hence  $\phi(0, -1/\sqrt{3}) = \sqrt{3}$ .
2. On  $\partial D$  we have  $g(b, b) = B\sqrt{5} \geq \sqrt{5}$ . Hence  $\min_{\partial D} \phi > \sqrt{3}$ .
3. As  $b^2 + t^2 \rightarrow \infty$  in  $D$ , we have  $f, g \rightarrow +\infty$ .

From these properties, we see that the global minimum of  $\phi$  is achieved at some point in the interior of  $D$ . Next, we compute

$$\frac{\partial f}{\partial t} = -1 + \frac{t}{T} < 0, \quad \frac{\partial g}{\partial t} = 1 + \frac{t}{4B^2 + T^2} > 0.$$

Hence the gradients of  $f$  and  $g$  are never zero, and are never positive multiples of each other. For this reason, any point where  $\phi$  achieves a global minimum lies on the set where  $f = g$ . ♠

Setting  $f = g$  and solving for  $b$ , we get

$$b = \beta(t) = \frac{t^3 - T^3 - 3t}{3t^2 - 1}. \quad (9)$$

There no solutions to  $f = g$  when  $t = +1/\sqrt{3}$  and Item 1 above (or a direct calculation) shows that  $\beta(-1/\sqrt{3}) = 0$ . In particular,  $\beta$  has a removable singularity at  $t = -1/\sqrt{3}$  and hence is smooth on the domain

$$D^* = (-\infty, 1/\sqrt{3}).$$

When  $t > 1/\sqrt{3}$  we have  $b = \beta(t) < 0 < t$ . Hence, only  $t \in D^*$  corresponds to points in  $D$ . So, we just need show  $\min_{D^*} \phi^* = \lambda_1$ , where

$$\phi^*(t) = f(\beta(t), t) = \frac{2T(t^2 - tT - 1)}{3t^2 - 1} \quad (10)$$

As  $t \rightarrow -\infty$  or  $t \rightarrow 1/\sqrt{3}$  we have  $\phi^*(t) \rightarrow +\infty$ . Hence  $\phi^*$  achieves its minimum on  $D^*$  at some point where  $d\phi^*/dt = 0$ . This happens only at

$$t_0 = -\sqrt{\frac{2}{\sqrt{3}} - 1} = -.39332\dots$$

We check that  $\phi^*(t_0) = \lambda_1$ .

## 4 Further Results

### 4.1 The Main Result

We state our result for immersed paper Moebius bands of aspect ratio less than  $\sqrt{3}$ . Thanks to Lemma 1.2, these results apply to any embedded examples, should they exist. Figure 4.1 shows a copy of Figure 3.1, with an extra vector  $(x, y)$  added in. This vector points from the right endpoint of the horizontal bend image to the midpoint of the vertical bend image.

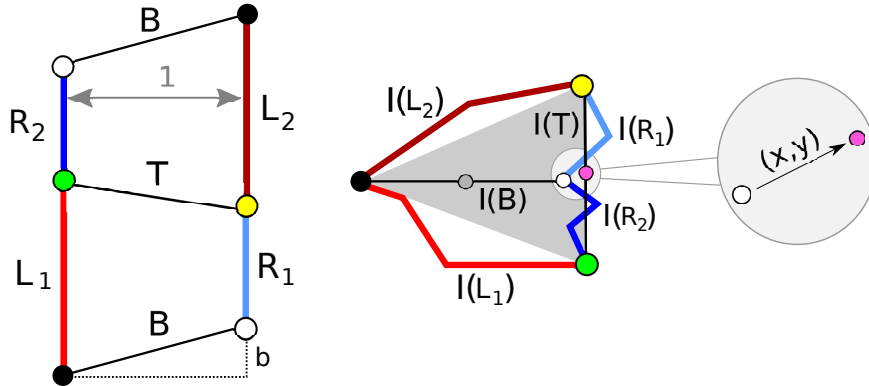


**Figure 4.1:** An elaboration of Figure 3.1.

Let  $\Delta$  be the (shaded) convex hull of the  $T$ -pattern  $I(T) \cup I(B)$ . Let  $S_j = L_j + R_j$  for  $j = 1, 2$ . The aspect ratio of our paper Moebius band is  $\lambda = (S_1 + S_2)/2$ . Theorem 1.1 gives a bound on this average. Now we give a bound on each sum  $S_j$  separately, and we also bound the geometry of  $\Delta$ .

**Theorem 4.1** *For any immersed paper Moebius with a  $T$ -pattern and aspect ratio less than  $\sqrt{3}$ , the following is true.*

1.  $S_j \geq \sqrt{3} - \frac{1}{3}b(1 - 2b)$  for  $j = 1, 2$ .
2.  $x < 1/18$  and  $|y| < 1/30$ .
3.  $\Delta$  is a triangle with minimum angle greater than  $\pi/4$ .

The function  $f(b) = \frac{1}{3}b(1 - 2b)$  has maximum value  $1/24$ . Hence we have  $S_j > \sqrt{3} - (1/24)$  for  $j = 1, 2$ . The corresponding bound for  $\lambda$  is only slightly weaker than the one in Theorem 1.1.

## 4.2 The Range of Slopes

We continue with the notation from the previous chapter. In particular, let  $f$  and  $g$  be the two constraint functions from §3.2 and let  $\phi = \max(f, g)$ . Again,

$$f(b, t) = b - t + T, \quad g(b, t) = -b + t + \sqrt{4B^2 + T^2}.$$

Here  $T = \sqrt{1 + t^2}$  and  $B = \sqrt{1 + b^2}$ .

Let  $\Omega$  be the set of values  $(b, t)$  satisfying  $\phi(b, t) < \sqrt{3}$ . We plot  $\Omega$  in Figure 4.1. These are the possible values  $(b, t)$  of slopes of bends which can participate in a  $T$ -pattern when the aspect ratio is less than  $\sqrt{3}$ .

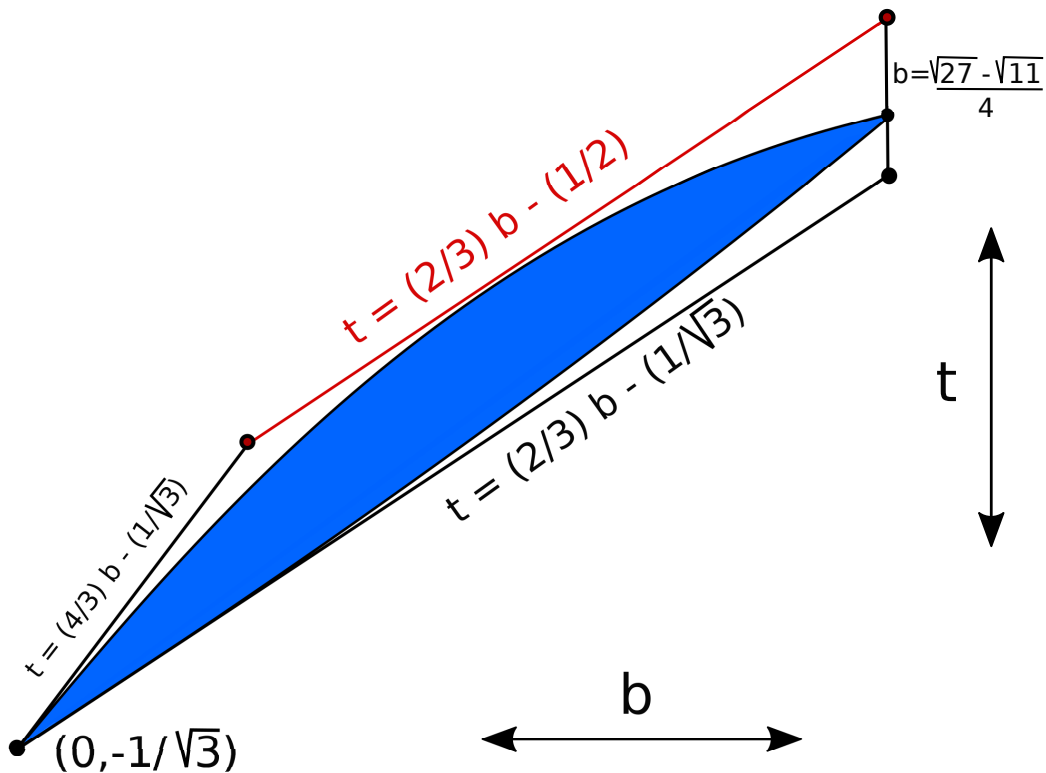


Figure 4.1: The range of slopes.

We have added in some points and lines to help frame  $\Omega$ , and in particular we have placed it inside a trapezoid which tightly hugs it. All the lines drawn touch  $\partial\Omega$  except the red one, which lies just barely above  $\Omega$ . The lines of slope  $2/3$  and  $4/3$  through  $(0, -1/\sqrt{3})$  are tangent to  $\Omega$ . The right vertex of  $\Omega$  is  $(a, -a/2)$  where  $a = (\sqrt{27} - \sqrt{11})/4 = .4698\dots$

**Lemma 4.2**  $\Omega$  is a subset of the trapezoid indicated in Figure 4.1.

**Proof:** We compute

$$\frac{\partial f}{\partial t} = -1 + \frac{t}{T} < 0, \quad \frac{\partial g}{\partial t} = 1 + \frac{t}{5 + 5b^2 + t^2} > 0$$

This calculation shows that the sets  $f = \sqrt{3}$  and  $g = \sqrt{3}$  are graphs of smooth functions. Call these graphs  $\Gamma_f$  and  $\Gamma_g$ . Let  $a = (\sqrt{27} - \sqrt{11})/4$ . We check algebraically that  $\Gamma_f$  and  $\Gamma_g$  intersect only at  $(0, -1/\sqrt{3})$  and  $(a, -a/2)$ . Moreover, we check that  $\Gamma_g$  lies below  $\Gamma_f$  at  $b = -1, 1$ . Hence  $\Gamma_g$  lies below  $\Gamma_f$  for all  $b \notin [0, a]$ . Given our derivative calculation, this shows that  $\Omega$  lies in the strip between the lines  $b = 0$  and  $b = a$ . Now we consider the 3 non-vertical constraint lines:

- We show that  $\Omega$  lies below the line  $t = (2/3)b - (1/2)$ . Since  $\partial g/\partial t > 0$  it suffices to prove that the restriction of  $g$  to our line is greater than  $\sqrt{3}$ . The minimum of  $g(b, (2/3)b - 1/2)$  occurs at  $b = (39 + \sqrt{8151})/520$  and the value there is about  $\sqrt{3} + .00002$ .
- We show that  $\Omega$  lies above the line  $t = (2/3)b - 1/\sqrt{3}$ . Since  $\partial f/\partial t < 0$  it suffices to show that  $f(b, (2/3)b - 1/\sqrt{3}) > \sqrt{3}$  for  $b > 0$ . We check that this is the case. The infimum occurs at  $b = 0$  and the value is  $\sqrt{3}$ .
- A similar argument, with  $g$  in place of  $f$ , shows that  $\Omega$  lies below the line  $t = (4/3)t - (1/\sqrt{3})$ .

This completes the proof. ♠

Here is a corollary.

**Theorem 4.3** If  $\mathcal{M}$  is an immersed paper Moebius band with a T-pattern and aspect ratio less than  $\sqrt{3}$  then  $\mathcal{M}$  has at least 2 bends that are perpendicular to the boundary of the Moebius band.

**Proof:** One thing we notice right away is  $(b, t) \in \Omega$  implies that  $b > 0$  and  $t < 0$ . That is, the bends have opposite slopes. Applying the Intermediate Value Theorem, we see that there are two bends that have slope 0. More geometrically, these bends are perpendicular to the boundary of the Moebius band. ♠

### 4.3 Another Constraint

We first establish another constraint imposed by Figure 3.1.

**Lemma 4.4**  $B^2 - L_j^2 + (T - R_j)^2 \leq 0$  for  $j = 1, 2$ .

**Proof:** We take the case  $j = 1$ . The case  $j = 2$  is the same, except that the vector  $(x, y)$  is replaced by the vector  $(x, -y)$ . We set  $L = L_1$ , etc.

Let

$$\Theta = (B/2 + x, y). \quad (11)$$

Let  $\Gamma$  be the portion of the ridge curve corresponding to  $\tau$ . Here  $\Gamma$  connects  $(B, 0, 0)$  to  $(0, T, 0)$ . Let  $\mu_1, \dots, \mu_n$  be the associated sign sequence. The  $(-)$  signs corresponding to the left side of the trapezoid  $\tau$  and the  $(+)$  signs correspond to the right. Let  $M_{\pm} \subset \{1, \dots, n\}$  denote those indices  $i$  such that  $\mu_i = \pm 1$ . Let  $\Gamma'_1, \dots, \Gamma'_n$  denote the edges of  $\Gamma$ . Let

$$L_{\text{str}} = \sum_{i \in M_-} \Gamma'_i, \quad R_{\text{str}} = \sum_{i \in M_+} \Gamma'_i. \quad (12)$$

It follows from the definitions that

$$\|L_{\text{str}}\| \leq L, \quad \|R_{\text{str}}\| \leq R, \quad R_{\text{str}} + L_{\text{str}} = (-B, T, 0), \quad R_{\text{str}} - L_{\text{str}} = 2\Theta. \quad (13)$$

See Equation 4 for the justification of the last inequality. Define

$$p = (B, 0, 0) + R_{\text{str}} = (0, T, 0) - L_{\text{str}} = \left( \frac{B}{2}, \frac{T}{2}, 0 \right) + \Theta. \quad (14)$$

Let  $\pi_k$  be projection onto the  $k$ th coordinate. We have  $\pi_1(p) = B + x$ . Also,

$$\pi_2(p) \leq \|R_{\text{str}}\| \leq R < 1 \leq T.$$

Set  $\zeta = (0, T, 0)$ . By the Pythagorean Theorem:

$$\|(B, R, 0) - \zeta\| \leq \|(B + x, \|R_{\text{str}}\|, 0) - \zeta\| \leq \|p - \zeta\| = \|L_{\text{str}}\| \leq L. \quad (15)$$

Hence  $\|(B, R) - (0, T)\| \leq L$ . Squaring both sides and rearranging, we get the advertised constraint. ♠

## 4.4 Proof of Statement 1

We pick an index  $j = 1, 2$  and then set  $L = L_j$ , etc. Plugging in Equation 8 into the constraint from Lemma 4.4, we see that this constraint is equivalent to

$$2 + b^2 + t^2 + bT - tT - S(b - t + T) \leq 0.$$

Rearranging this expression, we see that we must have

$$S \geq \psi(b, t) := \frac{2 + b^2 + t^2 + bT - tT}{b - t + T}. \quad (16)$$

Hence

$$S + \frac{b(1 - 2b)}{3} - \sqrt{3} \geq \hat{\psi}(b, t) := \psi(b, t) + \frac{b(1 - 2b)}{3} - \sqrt{3}. \quad (17)$$

Hence, it suffices to prove that  $\min_{\Omega} \hat{\psi} = 0$ , where  $\Omega$  is as in Figure 5.2.

The expression  $b - t + T$  is positive when  $b > t$ , which we have on  $\Omega$ . Using the solvable expression trick on  $(b - t + T)\hat{\psi}$ , we find that  $\hat{\psi}(b, t) = 0$  only if  $P(b, t) = 0$ , where  $P(b, t)$  is the following polynomial:

$$4b^6 - 8b^5t - 16b^5 + 20b^4t + 12\sqrt{3}b^4 + 12b^4 - 24\sqrt{3}b^3t - 8b^3t - 24\sqrt{3}b^3 - 8b^3 + 9b^2t^2 + 12b^2t + 30\sqrt{3}b^2t - 12\sqrt{3}b^2 + 59b^2 + 18bt^3 - 42bt - 12\sqrt{3}b + 27t^2 + 18\sqrt{3}t + 9$$

It suffices to prove that  $P > 0$  on  $\Omega$ .

The expression for  $P$  is a monster but it is cubic in  $t$ . Let  $Z$  be the segment which is the subset of the line

$$t = (2/3)b - (1/\sqrt{3}). \quad (18)$$

parametrized by  $b \in (0, 1/2)$ . Given the description of  $\Omega$  in Figure 3.1, every point of  $\Omega$  can be reached from a point of  $Z$  by travelling upwards on a vertical ray. So, to prove that  $P > 0$  on  $\Omega$  it suffices to prove that  $P''' > 0$  when  $b > 0$  and that  $P, P', P'' > 0$  on  $Z$ . Here we are taking derivatives with respect to  $t$  but then we will use Equation 18 to express the answer in terms of  $b$ .

We compute  $P''' = 108b$ , which is certainly positive when  $b > 0$ . We then compute other derivatives and restrict to  $Z$ :

$$P'' = 54 - 36\sqrt{3}b + 90b^2, \quad P' = b(12 + 12b + 28b^2 - 24\sqrt{3}b^2) + b^4(20 - 8b). \\ (3/4)P = b^2(21 - 12\sqrt{3} + 18b - 10\sqrt{3}b + 12b^2 - 8\sqrt{3}b^2 - 2b^2) + b^5(2\sqrt{3} - b) \quad (19)$$

On  $(0, 1/2)$ , every linear polynomial in sight is positive and, as can be checked by the quadratic formula, every quadratic polynomial is positive as well. Hence, the expressions in Equation 19 are all positive on  $(0, 1/2)$ . This completes the proof.

## 4.5 Proof of Statement 2

We can normalize by an isometry so that  $y \geq 0$ .

**Lemma 4.5**  $x < 1/18$ .

**Proof:** Let  $L'_2$  denote the length of the segment in Figure 4.1 joining the endpoints (yellow, black) of  $I(L_2)$ . Define  $R'_1$  similarly. From the Pythagorean Theorem,

$$L_2 \geq L'_2 = \sqrt{(B+x)^2 + (T/2+y)^2} \geq \sqrt{(B+x)^2 + T^2/4}. \quad (20)$$

Also, we have  $R_1 \geq R'_1 = T/2 + y \geq T/2$ . Define the function

$$f(b, t, x) = T/2 + \sqrt{(B+x)^2 + T^2/4} - \sqrt{3}.$$

Since  $L_2 + R_1 < \sqrt{3}$ , we can prove that  $x < 1/18$  by showing that  $f > 0$  on  $\Omega$ .

Every point in  $\Omega$  can be reached by following a downward-pointing vertical ray which starts on the segment

$$Z = \{(b, t) \mid t = (2/3)b - (1/2), b \in I\}, \quad I = (0, 1/2). \quad (21)$$

Since (clearly)  $\partial f / \partial t < 0$ , we just need to prove that  $\phi > 0$  on  $[0, 1/2]$ , where

$$\phi(b) = f(b, (2/3)b - (1/2), 1/18). \quad (22)$$

We check that  $\phi(0) > 0$ . So, we just have to show that  $\phi$  does not vanish on  $[0, 1/2]$ . The expression for  $\phi$  is an iterated radical. An expression of the form  $u + v\sqrt{w}$  vanishes only if  $u^2 - v^2w$  vanishes. Using this fact 3 times, to eliminate the iterated radical, we find that  $\phi(b) = 0$  only if the following polynomial vanishes.

$$379204871936 - 2821217402880b - 3788174241792b^2 + 59974706921472b^3 - 81516306161664b^4 - 11284439629824b^5 + 30126667530240b^6 - 2821109907456b^8$$

Any number of methods – e.g., Sturm Sequences – shows that this does not happen. The closest root is 0.624325.... ♠

**Lemma 4.6**  $|y| < 1/30$ .

**Proof:** We keep the notation from the previous lemma. We have

$$R_1 - y \geq R'_1 - y = T/2 \implies y \leq R_1 - (T/2).$$

Since  $x \geq 0$ , Equation 20 says that

$$L_2 \geq \sqrt{B^2 + (T/2 + y)^2}. \quad (23)$$

Since  $L_2 + R_1 < \sqrt{3}$ , we have

$$y \leq (R_1 + L_2) - L_2 - (T/2) < \sqrt{3} - \sqrt{B^2 + (T/2 + y)^2} - (T/2).$$

The last inequality comes from Equation 23.

Define

$$h(b, t, y) = \sqrt{B^2 + (T/2 + y)^2} + (T/2) + y - \sqrt{3} \quad (24)$$

To finish our proof it suffices to prove that  $h(b, t, 1/30) > 0$  on  $\Omega$ . The argument is just as in the previous case, except that now the final polynomial is

$$-300b^4 - 40\sqrt{3}b^2 + 1600b^2 - 600b + 80\sqrt{3} - 79.$$

This polynomial has two negative roots and two non-real roots. ♠

## 4.6 Proof of Statement 3

Since  $|y| < T/2$ , the convex hull  $\Delta$  is a triangle. Now we consider the angles. To make the numbers easier, all we use is that  $x < 1/18$  and  $|y| < 1/8$ .

The (vertical) base of  $\Delta$  has length  $T = \sqrt{1 + t^2}$ . The (horizontal) altitude of  $\Delta$  has length  $B = \sqrt{1 + b^2} + x$ . Let  $\alpha$  be the foot of the altitude and let  $\beta$  be the midpoint of the base. We have  $|t| < 1/\sqrt{3}$  on  $\Omega$ . Hence  $\Delta$  has base length less than  $5/4$ . Since  $\|\alpha - \beta\| = |y| < 1/8$ , the foot  $\alpha$  is at most  $3/4$  from either the top or bottom vertex. The altitude has length at least 1. Hence, both top and bottom angles exceed

$$\tan^{-1}(4/3) > \pi/4.$$

Now we consider the angle at the left vertex. The function  $f(b, t) = (B + \frac{1}{18})/T$  is maximized at the right vertex of  $\Omega$  and its value there is  $1.129\dots < 1.13$ . Hence, the altitude/base ratio of  $\Delta$  is at most 1.13. At the same time, the base length is at least 1 and (again)  $\|\alpha - \beta\| < 1/8$ . Hence, the left angle of  $\Delta$  is at least

$$\tan^{-1}\left(\frac{3/8}{1.13}\right) + \tan^{-1}\left(\frac{5/8}{1.13}\right) = (1/4) \times 3.30\dots > \pi/4.$$

This completes the proof.

## 5 References

[AHLM] A. Malaga, S. Lelievre, E. Harriss, P. Arnoux,  
*ICERM website: <https://im.icerm.brown.edu/portfolio/paper-flat-tori/>* (2019)

[CB], R. Connolly, A Back, *Mathematics and Tensegrity*, in **American Scientist**, Vol 82 **2**, (March-April 1998) pp 142-151.

[CF] Y. Chen and E. Fried, *Möbius bands, unstretchable material sheets and developable surfaces*, Proceedings of the Royal Society A, (2016)

[CKS] J. Cantarella, R. Kusner, J. Sullivan, *On the minimum ropelength of knots and links*, Invent. Math. **150** (2) pp 257-286 (2003)

[FT], D. Fuchs, S. Tabachnikov, *Mathematical Omnibus: Thirty Lectures on Classic Mathematics*, AMS 2007

[HF], D.F. Hinz, E. Fried, *Translation of Michael Sadowsky's paper 'An elementary proof for the existence of a developable Möbius band and the attribution of the geometric problem to a variational problem'*. J. Elast. 119, 3–6 (2015)

[HW], B. Halpern and C. Weaver, *Inverting a cylinder through isometric immersions and embeddings*, Trans. Am. Math. Soc **230**, pp 41.70 (1977)

[MK] L. Mahadevan and J. B. Keller, *The shape of a Möbius band*, Proceedings of the Royal Society A (1993)

[Sa], M. Sadowski, *Ein elementarer Beweis für die Existenz eines abwickelbaren Möbiusschen Bandes und die Zurückführung des geometrischen Problems auf ein Variationsproblem*. Sitzungsberichte der Preussischen Akad. der Wissenschaften, physikalisch-mathematische Klasse 22, 412–415.2 (1930)

[S1] G. Schwarz, *A pretender to the title “canonical Moebius strip”*, Pacific J. of Math., **143** (1) pp. 195-200, (1990)

[S2] R. E. Schwartz, *The 5 Electron Case of Thomson's Problem*, Journal of Experimental Math, 2013.

[W] S. Wolfram, *The Mathematica Book, 4th Edition*, Wolfram Media and Cambridge University Press (1999).